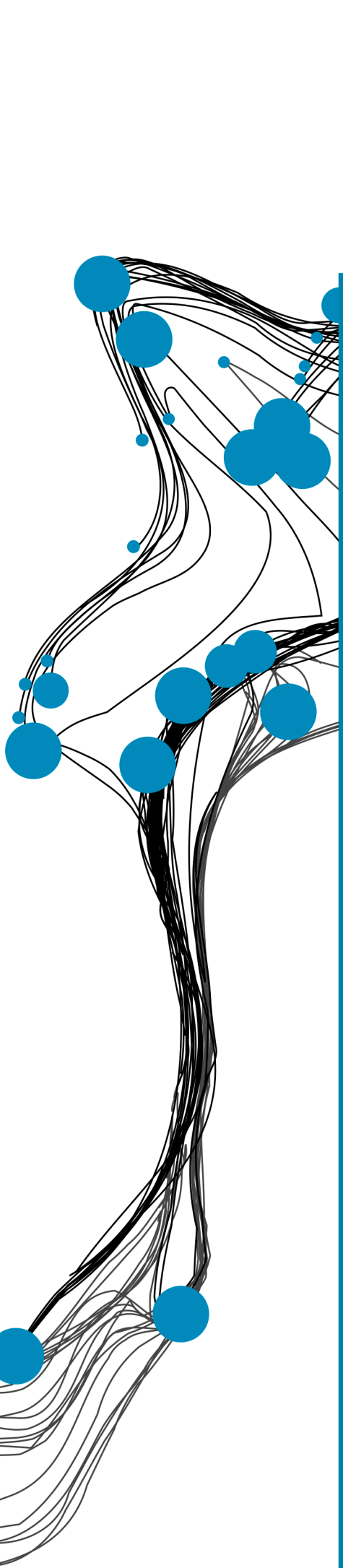

University of Twente

BSc Assignment

Applying sensor calibration and minimizing gyroscopic drift of the Madgwick filter from IMU data from patients the first 24 hours after a DMEK

L.C.M. Te Brake

Comittee:
Chair: B.J.F. Van Beijnum
Supervisor: S.J. Mevissen
External member: J.A.M. Haarman

April 26, 2024

Abstract

DMEK is a treatment option for patients who suffer from Fuchs' endothelial dystrophy. During the procedure, a part of the patient's cornea is removed. The transplant is placed with an air bubble. During the first 24 hours after the surgery, patients are instructed to remain supine. The influence of this instruction on the risk of graft detachment is researched. This is done with an IMU placed on the forehead of the patient. The orientations of the head are retrieved from the IMU's gyroscope and accelerometer data with the help of the Madgwick filter. After the use of this filter, a gyroscope drift is observable. This drift shows movement while the sensor is stationary. It was attempted to eliminate the drift using an IMU sensor calibration and a linear regression algorithm. The calibration has a significant impact on reducing the gyroscope drift. Additionally, the linear regression slightly reduces the gyroscope drift. Unfortunately, a slight drift was still visible in the yaw angles. When the linear regression model was applied to the patient data, it did not work. Thus, the linear regression model cannot be applied to patient data. Another filter which could be applied to eliminate the yaw drift is the NMNI filter.

Samenvatting

DMEK is een behandeling voor mensen met Fuchs' endotheel dystrofie. Tijdens de operatie wordt een deel van het hoornvlies verwijderd. Het donor hoornvlies wordt geplaatst met behulp van een luchtbubbel. De eerste 24 uur na de operatie worden de patiënten geïnstrueerd om zoveel mogelijk plat te liggen. Er wordt onderzocht in hoeverre deze instructie invloed heeft op de loslating van het transplantaat. Hiervoor wordt de eerste 24 uur een IMU die bewegingen van het hoofd meet op het voorhoofd van de patiënt geplaatst. De oriëntaties van het hoofd worden berekend door het Madgwickfilter aan de hand van de gyroscoop en accelerometer data van de IMU. In de berekende oriëntaties is nog een afwijking (drift) zichtbaar. Deze drift zorgt voor een beweging in de data, terwijl de sensor zelf stil ligt. Er is geprobeerd de drift te verwijderen door sensor kalibratie gecombineerd met een lineair regressie model. De sensor kalibratie heeft de drift significant verminderd. Het lineaire regressie model vermindert de drift minimaal. Er is echter nog een drift zichtbaar in de yaw hoeken. Na het toepassen op de patiënt data bleek dat het lineaire regressie model niet werkt op patiënt data. Een filter wat de resterende drift van de yaw hoeken zou kunnen oplossen is het NMNI filter.

Contents

1 Introduction

Worldwide, 300 million people over the age of 30 suffer from Fuchs' endothelial corneal dystrophy (FECD). This number is expected to increase by almost 50% in 2050. [1] FECD affects the corneal endothelium of the eye. Patients who suffer from FECD experience a progressive degeneration of the corneal endothelium. The Descemet membrane thickens due to corneal edemas. Additionally, the membrane contains focal endothelial excrescences, which are called guttae. Patients experience reduced vision and other symptoms which are associated with glare. The symptoms are experienced more intensely during and shortly after awakening. As the disease progresses fluid filled sacks or lesions, also called bullae, appear. Rupture of these can result in pain episodes. In the last stage scar tissue appears on the cornea, which lessens the formation of bullae, but reduces the vision. [2] Other symptoms patients experience include photophobia and an overflow of tears. [3]

One of the treatment options for FECD is an endothelial keratoplasty. During these procedures (a part of) the cornea (figure 1) is transplanted. [3] A specific endothelial keratoplasty technique used for patients who suffer from FECD is Descemet membrane endothelial keratoplasty (DMEK). The donor graft used during this procedure consists of the Descemet membrane and the corneal endothelium (figure 1). The graft is placed and positioned with the help of an air bubble. [5]

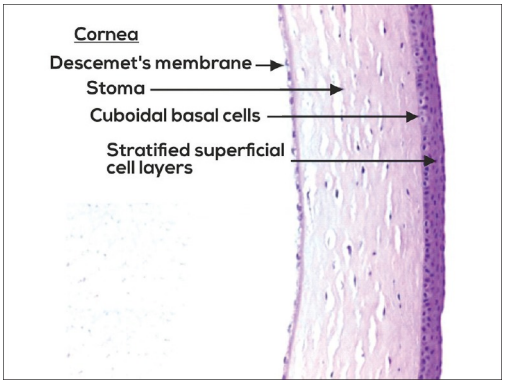

Figure 1: The different layers of the cornea are shown. The corneal endothelium is located on the left side of the Descemet's membrane. [4]

During the past years, DMEK has become a standard treatment option for FECD. [6] After surgery patients are instructed to remain in a mostly flat (supine) position for at least 24 hours after surgery. It is presumed that this instruction promotes graft attachment as the air bubble will rise and press the graft to the recipient's cornea. [7] However, recent studies question the need for supine posturing after a DMEK procedure. These studies show no significant increased risk of graft detachment without supine posturing after DMEK. [8, 9]

This report is a part of the Eye in the Sky project (EITS). EITS is a collaboration between Deventer Ziekenhuis and the University of Twente. The project researches the influence of head positions and movements on graft detachment in the first 24 hours after a DMEK. The movements of patients during the first 24 hours after a DMEK are tracked using an inertial measurement unit (IMU). This IMU is placed on the forehead of the patient. It is assumed head orientations are equal to eye orientations. The IMU sensor is placed in the operating room directly after the DMEK procedure has been performed. The patients wear the IMU for the first 24 hours post-surgery. During the checkup, 24 hours post-operatively, the sensor is removed from the patient's head and the data can be saved and analysed. This report focuses on a part of the data analysis of the retrieved data.

During previous research, the orientation of the head was retrieved from the IMU data. This was done with the Madgwick filter. [10] However, after application of the Madgwick filter a drift was present in the calculated head orientations. This drift causes a show of movement in the orientations, while the sensor is stationary in real life. The drift is caused by the gyroscopic data of the IMU. This drift is called the gyroscope zero bias. The name refers to the bias the gyroscope data shows, while the sensor is stationary and the gyroscope values should be zero. This report focuses on the elimination of the gyroscopic drift to retrieve correct head positions. This leads to the research question:

To what extent can the gyroscope drift of IMUs be corrected with sensor calibration and a linear regression model?

2 Background

2.1 Patient procedure

In this project the type of endothelial keratoplasty, which is performed on the patients, is DMEK. During the DMEK procedure, the Descemet membrane of the recipient's eye is stripped from the stroma in a circular shape and taken out of the eye. During donor preparation, the donor membrane is stained to increase its visibility in the recipient's eye during the placement of the graft. The donor Descemet membrane is inserted in the recipient's eye through an incision. Next, the donor membrane is unfolded and positioned against the recipient's stroma. Lastly, the membrane of the donor is adhered to the corneal stroma of the recipient with the help of an air bubble. During half an hour the anterior chamber is filled with air. After this half-hour, part of the air is released from the eye (figure 2). [5] An air bubble is left in the eye to promote graft attachment.

After the execution of the DMEK procedure, the sensor is attached to the forehead of the patient with the help of tape. The patient is laid flat (supine) in the bed with the eyes and head pointed to the ceiling. Patients are instructed to stay in a supine position until the next checkup, 3 hours after the surgery. The following 21 hours the patients are requested to be in a supine position to the maximum extent possible. A supine position is thought to promote graft attachment as the air bubble will push the graft to the recipient's cornea during a supine position. 24 hours after the end of the surgery another checkup with the doctor has been scheduled and the sensor is removed from the patient's forehead. The measurement is ended and the data are saved.

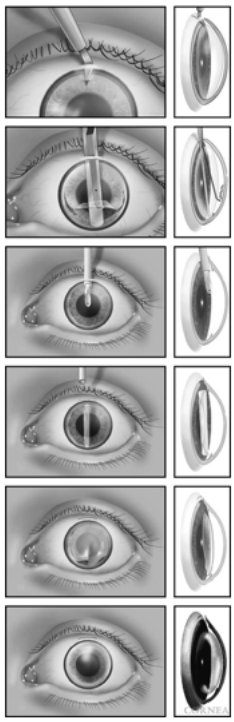

Figure 2: The different steps of a DMEK procedure are shown. [5]

2.2 Inertial measurement unit

The sensors used in this project are IMUs. These sensors contain gyroscopes and accelerometers to measure the angular velocity and linear acceleration along three axes (x, y and z) (figure 3a). [11] IMUs may contain magnetometers, these were however not present in the sensor used for this project. The IMU measures the sensor's orientation relative to the starting position of the measurement of the sensor.

IMU sensors are self-contained. [11] This implies that patients who have this sensor attached to their head can move freely, without being constrained by for example cables or reception ranges. This causes the behaviour of the patients to be minimally affected by the sensor.

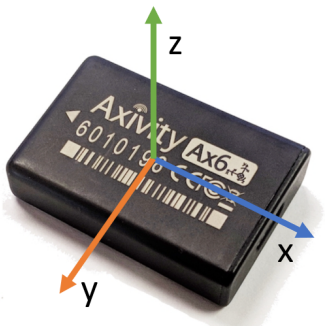

(a) The different axes of the sensor frame of the IMU are depicted. Blue: x-axis, red: y-axis, green: z-axis.

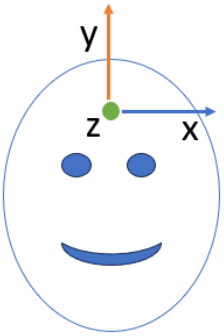

(b) The frame of the head is shown. The green dot refers to the z-axis coming out of the forehead of the head. The blue and red arrows are the x- and y-axis respectively.

Figure 3: The two orientation frames that are used in this report are shown; on the left, sensor frame (a) and on the right, the head frame (b) are depicted.

2.2.1 Orientation frames

In this project two orientation frames are present; the sensor frame and the head frame. The sensor's frame consists of the coordinate system (x-, y- and z-axis) of the sensor itself (figure 3a). The head frame is the x-, y- and z-axis coordinate system on the forehead of the patient. Here the z-axis comes straight out of the forehead of the subject, the x-axis goes through the ears and the y-axis comes out of the top of the head (figure 3b). To transform the orientations in the sensor frame to the head frame, a rotation matrix is needed. This rotation matrix was determined with the help of a bed calibration performed right after placing the sensor on the patient's head.

In this project, the rotation angles around a specific axis are used as a parameter to express the head orientation and rotation. These angles are called, the roll, pitch and yaw angles (figure 4). The roll angles correspond to the rotations around the x-axis. When applying this to the head orientations, the rotations are similar to nodding yes. The pitch angles correspond to the rotations around the y-axis. These rotations are similar to shaking no in the head frame. The yaw angles correspond to the rotations around the z-axis. In the head frame, these rotations are caused by movements similar to moving the ears to the shoulder.

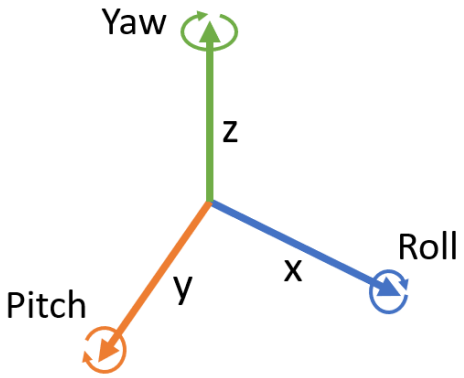

Figure 4: The used rotation angles are shown. Roll refers to rotations around the x-axis (blue). Pitch angles refer to rotations around the y-axis (red). Yaw angles refer to rotations around the z-axis (green).

2.3 Madgwick filter

During previous research, the data of the IMUs was processed with the help of a Madgwick filter. This filter is applicable for relatively low sampling frequencies and has a lower computational load than similar filters (e.g. Kalman). The filter calculates the estimated quaternion orientation from the data of the accelerometers and gyroscopes. [12] From this filter the roll, pitch and yaw angles are retrieved. [10] When using this filter a gyroscope drift is observed. This drift results in a show of movement, while the sensor is stationary. [10, 12] This drift can be observed clearly in the yaw angles of figure 5. These yaw angles are the angles of a stationary sensor in a known position. At the start of the measurement, a deviation can be seen in all three angles by the slopes present. Furthermore, the roll angles show a significant rise to 180°, while the sensor is stationary. Lastly, the yaw angles show a mostly constant linear decrease. This report focuses on eliminating this drift.

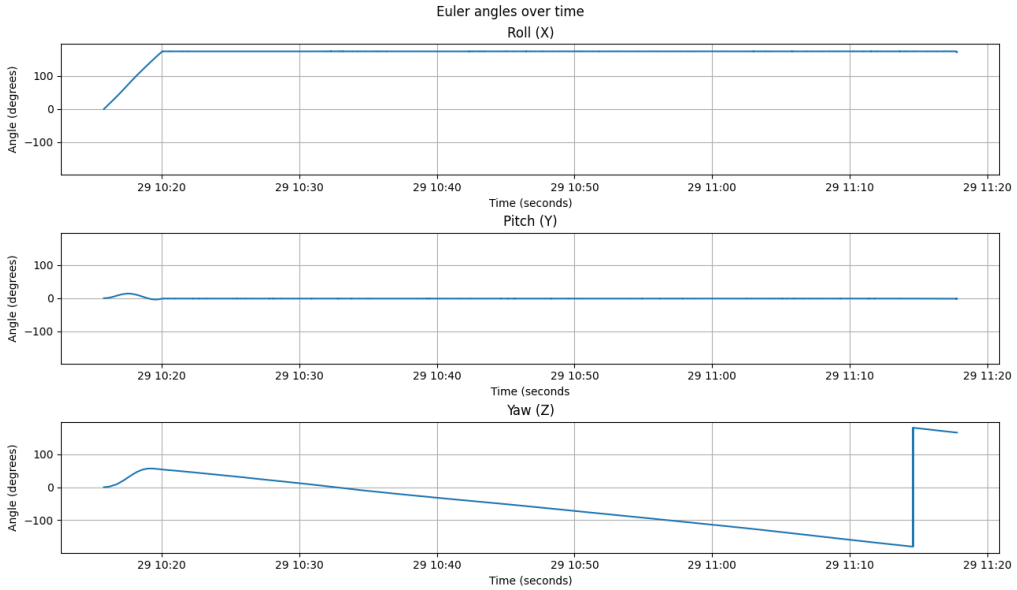

Figure 5: The angles of a sensor which has been stationary for one hour are shown. From top to bottom; the roll, pitch and yaw angles are depicted.

2.4 Eliminating drift

As explained in section 2.3 a drift occurs in the calculation of the orientation. Two ways of eliminating this drift are the no motion no integration (NMNI) algorithm and a linear regression model. These models have already been applied to IMU sensors without magnetometers. [13, 14] The NMNI algorithm has already been used in combination with the Madgwickfilter. This combination shows promising results for elimination in the drift of the yaw angles. The NMNI filter uses a constant gyroscope zero bias, which is updated during stationary periods to predict the bias in moving periods. [13] The linear regression algorithm, proposed by O-larnnithipong et al. is used to eliminate the drift in a hand tracking device. This model, like the NMNI filter, predicts the bias during stationary periods. However, the predicted bias is dependent on the time in the linear regression model. Additionally, this model focuses on all three (roll, pitch and yaw) angles. [14] In this project, the linear regression algorithm will be implemented, as this algorithm changes the bias over time and shows promising results for the tracking of body parts.

3 Methods

In this project, sensor calibration is applied to the accelerometer and gyroscopic data from the IMU. Then, a linear regression model is applied to the gyroscopic data to eliminate gyroscopic drift. Lastly, the Madgwick filter is applied to obtain orientations (figure 6). The results of the sensor calibration and linear regression model are validated by calculating the root mean square error (RMSE) of the different orientations from the Madgwickfilter. Finally, sector plots of the patients' data are determined.

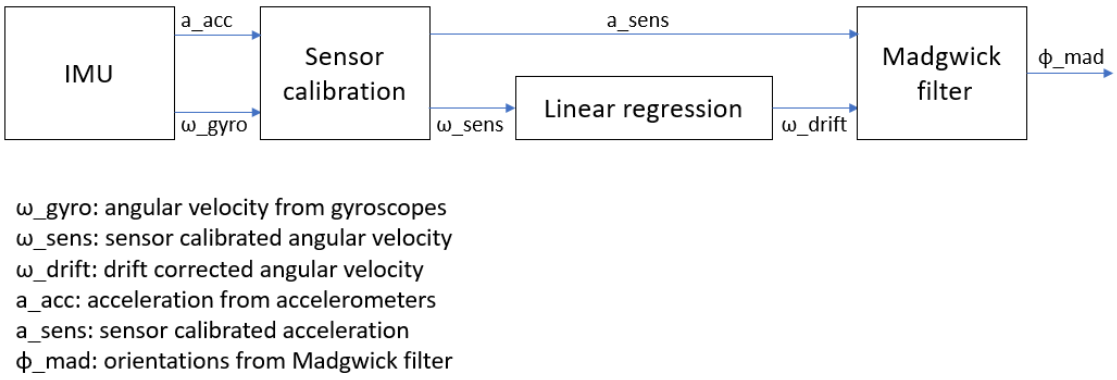

Figure 6: Overview of the calibrations and filters applied to the data.

3.1 Sensor calibration

The model of the IMU sensors used is Axivity AX6. The IMU measurements were performed and saved using OmGui software. During the measurements a sampling frequency of 200 Hz and a range of ±8 g and ± 1000 deg/s for the accelerometers and gyroscopes respectively were used. In the EITS project, multiple sensors are used for the retrieval of patient data. Per patient, only one sensor was used. For these sensors, the calibration values were determined. For each sensor, the sensor was attached to a hollow cube-like object with the help of tape (figure 7). The cube was placed in the starting position, which was marked with tape to ensure the sensor's position at the beginning and end of the measurement were identical. The rotations were performed manually. During the measurement, the sensor was twisted around the z-axis for 360° (green arrow) and returned to the starting position. After a stationary period of a couple of seconds, the sensor was tilted with 90° around the y-axis (red arrow). Then the sensor was tilted back to the starting position. Lastly, the sensor was tilted 90° and back around the x-axis (blue arrow). The movements during the measurements were identical for all the sensors used in the project.

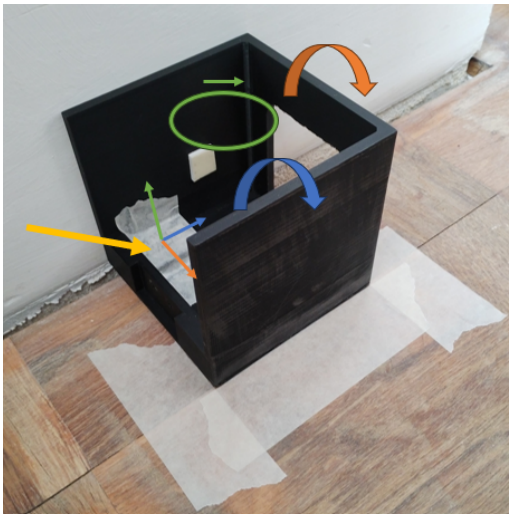

Figure 7: This cube and its marked starting position were used for the sensor calibration measurements. The location of the sensor is indicated by the yellow arrow. Additionally, the sensor's frame is shown. The coloured arcs are the rotations around the corresponding axes (90°, 90° and 360° for the x-, y- and z-axis respectively).

The bias and gain of both the accelerometers and gyroscopes were needed to calibrate the sensor. The bias is the fixed error which is subtracted from the sensor's output signal. The gain describes the factor with which the sensor output of the rotation is multiplied to deliver the actual rotation after the bias of the sensor has been compensated. The bias of the gyroscope and the bias and gain of the accelerometers were known. The gain of the gyroscope was calculated according to equation (1). Here, ϕ_{sensor} is the angle which is obtained from integrating the gyroscope data after the gyroscope bias has been subtracted from the data. Thus, this angle has been obtained by the measurement. Consequently, ϕ_{actual} is the actual angle the sensor has made, which was measured manually during the measurement. [15]

$$gain = \frac{\phi_{sensor}}{\phi_{actual}} \tag{1}$$

To apply the sensor calibration to the data, first, the bias of both the accelerometers and the gyroscopes was subtracted from the data. Next, the data was multiplied by the corresponding gains. Thus, the sensor calibration has been completed.

3.2 Linear regression model

The linear regression model was used to determine the gyroscope zero bias. It is important to note that this bias is different from the sensor's bias, which is described above in section 3.1. The gyroscope zero bias occurs when the sensor is stationary, but the gyroscope values are not zero. Thus the data shows movement, while the sensor is stationary. The linear regression model aims to predict the gyroscope zero bias with the help of stationary periods. During these stationary periods, the gyroscope zero bias is known, as the measured gyroscopic values are the bias. Equation (2) shows the mathematics of the linear regression model. The gyroscope zero bias b was calculated with coefficients α and β over time t. The coefficients, α and β, can be calculated using equations (3) and (4) respectively. In these equations, b_i and t_i resemble the measured gyroscope bias and time, respectively. Additionally, $\bar{b}$ and $\bar{t}$ correspond to the mean bias and mean time of one stationary period. [14] The coefficients α and β and the corresponding biases are determined for every stationary period.

$$b = \alpha + \beta t \tag{2}$$

$$\alpha = \bar{b} - \beta \bar{t} \tag{3}$$

$$\beta = \frac{\sum_{i=1}^{n}(t_i - \bar{t})(b_i - \bar{b})}{\sum_{i=1}^{n}(t_i - \bar{t})^2} \tag{4}$$

Per stationary period, the bias was subtracted from the gyroscopic data. The application of the bias during non-stationary periods is explained through figure 8. This figure shows a schematic example of gyroscopic

data. The bias for the stationary parts (indicated with the orange arrows) was calculated as described above (equation 2). For the non-stationary parts of the data (indicated with the blue arrow), the mean of the bias of both stationary periods was calculated, in this case, parts 1 and 2. Then this mean was subtracted from the gyroscopic values of the data. This has been done for the whole data set.

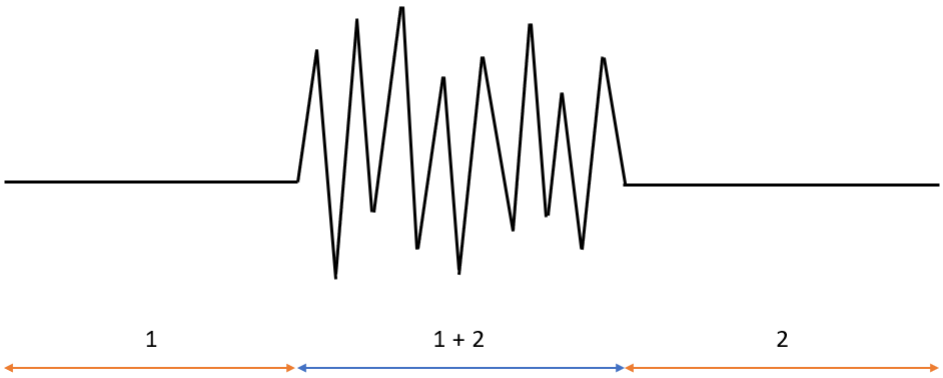

Figure 8: Schematic view of a part of the gyroscopic data.

The data used to evaluate the linear regression model was obtained with the same type of sensors and settings as described in section 3.1. The measurements were 7 and 8 hours long. Every hour, the sensor was stationary for 5 minutes in the known starting position. As explained above, stationary periods are needed to determine the gyroscope zero bias. To determine the stationary periods in the data, the unfiltered and uncalibrated gyroscopic data was plotted. Next, the stationary periods are selected manually. These periods are then saved and used later on to apply the linear regression model.

3.3 Root mean square error

The root mean square error (RMSE) was used to evaluate the influence of the sensor calibration and the linear regression model on the gyroscopic drift of the unfiltered data. The RMSE can be calculated using the following equation: [16]

$$RMSE = \sqrt{\frac{\sum_{i=1}^{n}(y_i - \hat{y}_i)}{n}} \tag{5}$$

Here, y_i represents the yaw, roll or pitch angle obtained by the Madgwick filter. Consequently, $\hat{y}_i$ represents the actual (known) angle of the sensor. In this application, the RMSE was calculated during stationary periods. It was known that the angles of the stationary periods were $0°$, as the stationary position was equal to the starting position. Hence, the RMSE equation was simplified (equation (6)).

$$RMSE = \sqrt{\frac{\sum_{i}^{n}(y_i)}{n}} \tag{6}$$

Using equation (6) the RMSE for the roll, pitch and yaw angles was calculated. To get an overview of the general result of the influence of the sensor calibration and the linear regression on the drift, the RMSE values of the roll, pitch and yaw angles were summed.

3.4 Sector plots

For the sector plots, patient data was used, compared to the data used in sections 3.1 and 3.2. To evaluate the orientations of the head of the patient during 24 hours sector plots were used. These plots display the amount of time spent in a specific orientation sector relative to the starting position with the help of a colour scale (figure 9). [10] The outer ring of the sector plot shows a rotation of more than 90° to any side, the second outer ring a rotation between 60° and 90°, the second inner ring between 30° and 60° and the inner ring a rotation of less than 30°. The labels 'X-axis' and 'Y-axis' refer to the rotational axis. Thus, a pure rotation of 90° around the y-axis would show activity in the most left or the most right part of the sector plot depending on the direction of rotation.

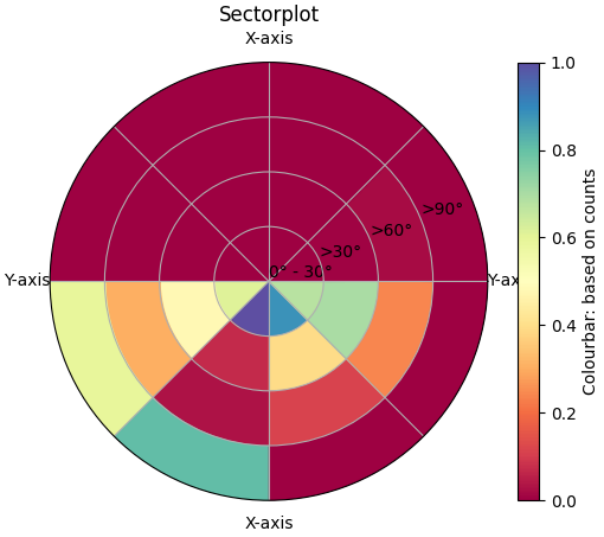

Figure 9: An example of a sector plot is shown.

The sector plot shows the xy-plane. For this plot, the z-axis from the head orientation is projected on the xy-plane. This was done using equation 7. This vector is then expressed in polar coordinates. The angle θ is expressed relative to the x-axis. Using these coordinates the vector can be assigned to a sector. The amount of projected z-vectors per sector is counted. The counts per sector are then normalized relative to the sector with the most counts and plotted.

$$v_p = v - \frac{v \cdot n}{||n||^2} \cdot n \tag{7}$$

4 Results

The linear regression coefficients α and β of 2 different measurements performed with the same sensor are shown and compared. Furthermore, the influence of the sensor calibration and linear regression model on the gyroscopic drift is discussed. Roll, pitch and yaw angles and their RMSE values are shown and evaluated. Lastly, the sensor calibration and linear regression are evaluated with the help of patient data depicted in sector plots.

4.1 Linear regression variables

In this section, two data sets (7-hour and 8-hour) are used to compare the variables (α and β) from the linear regression model. These datasets are retrieved by the same sensor and the α and β values are calculated at the same time in the measurement. For example, the second α_x value from the 7-hour dataset corresponds with the second α_x value from the 8-hour dataset. The procedure for these measurements is described in section 3.2. In table 1 it can be seen that corresponding α values show some similarities. However, some corresponding values differ slightly.

Table 1: The values of α are shown for every axis of the gyroscope. Both the values of 7-hour data and 8-hour data are shown.

7-hour			8-hour		
α_x	α_y	α_z	α_x	α_y	α_z
0.0237	-0.0501	-0.0225	0.0238	0.0534	-0.0299
-0.2709	-0.0453	0.0121	-0.2009	0.0057	0.0557
-0.3016	-0.2164	0.0736	-0.3625	-0.2187	0.1050
-0.3510	-0.3491	-0.0134	-0.3824	0.4297	-0.4334
0.2233	-0.0116	-0.1732	0.3627	0.5548	-0.1247
0.6896	-0.3107	-0.6959	0.4570	5.5032e-5	-0.3450
-0.6606	0.8591	-1.4947	0.1380	-0.6263	-0.0687
0.4772	-0.1766	-0.9448	0.6133	1.1673	-0.5709
n.a.	n.a.	n.a.	-0.5499	-1.2417	-0.4239

In table 2 it can be seen that the corresponding β values significantly differ. However, it should be taken into account that the values are very small (10^{-5}). Consequently, the influence of the β values on the bias determined by the linear regression model is minimal.

Table 2: The values of β are shown for every axis of the gyroscope. The values for the 7- and 8-hour data are shown.

7-hour			8-hour		
β_x	β_y	β_z	β_x	β_y	β_z
1.8239e-5	-4.1874e-5	-2.3899e-5	-1.3491e-5	-9.8929e-5	4.4417e-5
7.8139e-5	1.8730e-5	-9.0911e-6	5.7478e-5	4.0479e-6	-1.9981e-5
4.2285e-5	3.2165e-5	-1.2726e-5	4.3800e-5	3.0382e-5	-1.7374e-5
3.3184e-5	3.3650e-5	-8.2319e-7	3.5425e-5	-3.7748e-5	3.6801e-5
-1.4037e-5	2.4829e-5	1.0417e-5	-2.3597e-5	-3.6715e-5	6.5174e-6
-3.6938e-5	1.8454e-5	3.6860e-5	-2.4467e-5	1.3873e-6	1.7350e-5
3.1036e-5	-3.8172e-5	6.7266e-5	-5.5297e-6	2.9617e-5	1.8842e-6
-1.7975e-5	7.9144e-6	3.6093e-5	-2.3238e-5	-4.4620e-5	2.1254e-5
n.a.	n.a.	n.a.	1.2959e-5	4.3598e-5	1.3711e-5

4.2 Roll, pitch and yaw angles

The sensor calibration and linear regression model are evaluated using the roll, pitch and yaw angles from different data. Furthermore, the RMSE is used to further evaluate the sensor calibration and the linear regression model.

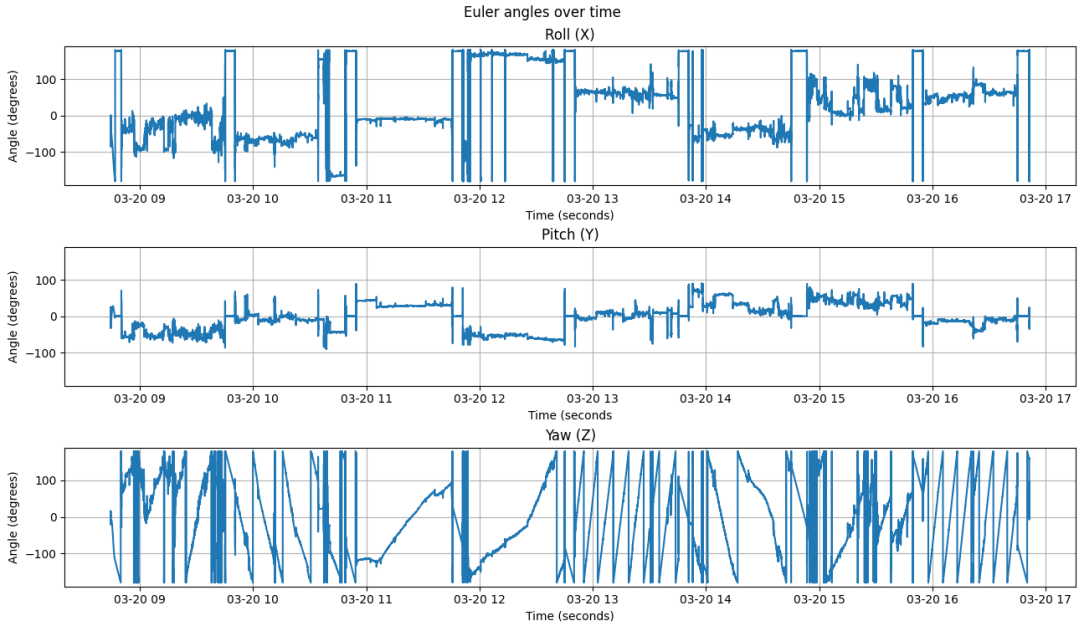

Figure 10: The roll, pitch and yaw angles of unfiltered data are shown. The saw tooth pattern of the yaw angles shows a drift with a steep slope.

In the figures 10, 11 and 12 the roll and pitch angles do not show any drift as there are no significant slopes distinguishable when compared to the yaw angles. The vertical lines from -180° to 180° are caused by a 'jump' from -180° to 180°. Figure 10 shows unfiltered data. Here, the drift in the yaw angles is visible in the form of the saw tooth pattern. This pattern is caused due to a steep slope and the 'jumps' from -180°to 180°.

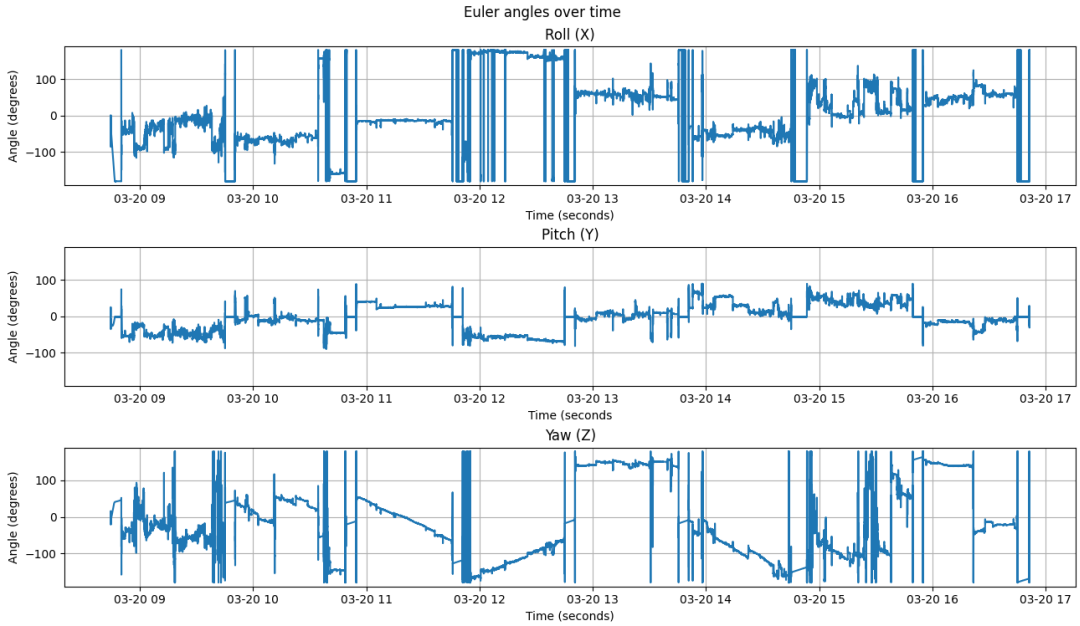

Figure 11: The roll, pitch and yaw angles of sensor-calibrated data are shown. A drift is visible in the yaw angles. This is shown by the slope of the angles.

Figure 11 shows the angles of the sensor calibrated data. Compared to figure 10 the drift has decreased, as no saw-tooth pattern is present. However, a drift is still present, due to the slope of the angles.

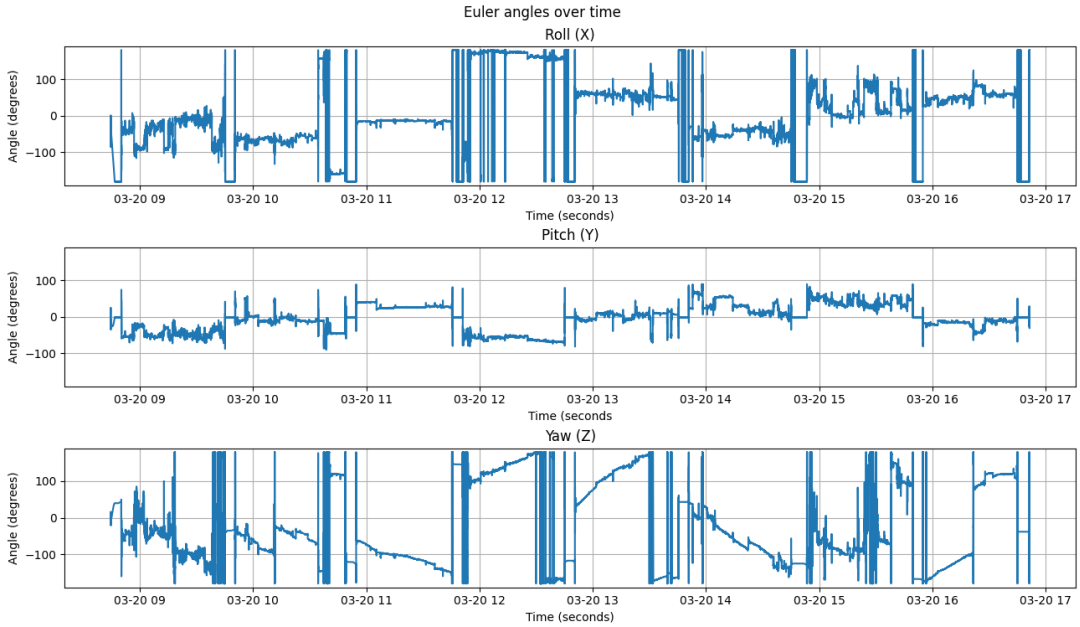

Figure 12: The roll, pitch and yaw angles of data that is sensor calibrated and filtered by the linear regression model are shown. A drift is visible in the yaw angles. This drift is shown by the slope of the angles.

Figure 12 shows the data that has been sensor calibrated and filtered with the linear regression model. With close inspection of figures 11 and 12, it can be observed the drift has been slightly minimized. This is visible by a slight decrease in the slope of the angles.

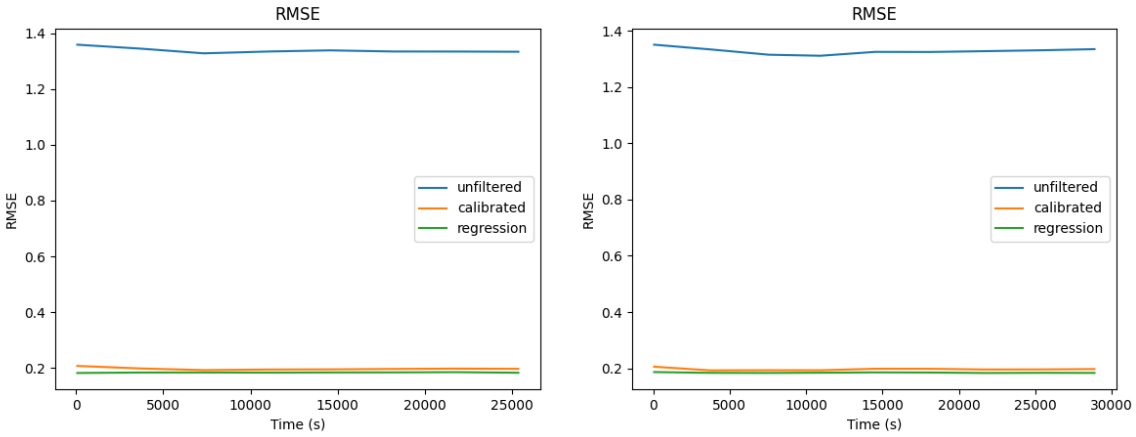

(a) The RMSE of the unfiltered (blue), sensor calibrated (red) and sensor calibrated and filtered (green) 7-hour data are shown.

(b) The RMSE of the unfiltered (blue), sensor calibrated (red) and sensor calibrated and filtered (green) 8-hour data are shown.

Figure 13: The RMSE according to the duration of the measurement are shown for the 7-hour data (a) and 8-hour data (b).

When inspecting the RMSE of the 2 different data sets (figure 13), it can be seen that the sensor calibration of the data significantly decreased the RMSE of the stationary periods of the data. Furthermore, a slight decrease in the RMSE of both data sets can be identified after applying the linear regression model to the sensor-calibrated data.

4.3 Sector plots

Sector plots made using patient data are shown. The same patient data was used for every sector plot. The influence of sensor calibration and linear regression model on the data is evaluated.

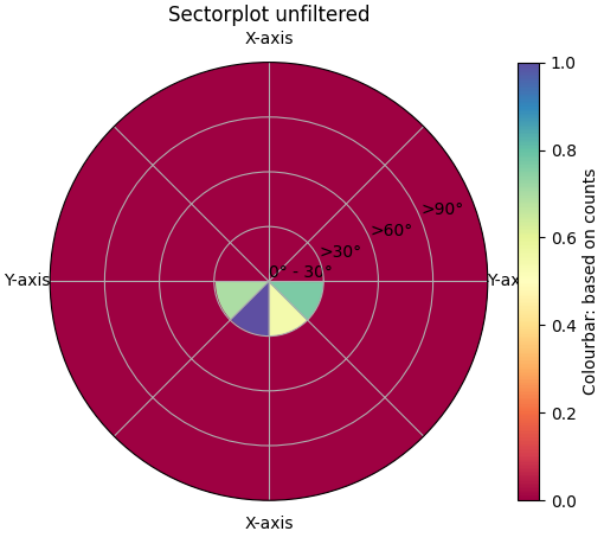

Figure 14: The sector plot of unfiltered patient data of the first three hours after the surgery is shown. It can be seen that the patient was in a supine position.

In figures 14, 15 and 16 the first 3 hours of the patient data are shown in a sector plot. As described in section 2.1, the patient was still in the hospital and mostly in a supine posture. This is visible in figures 14 and 15 as most of the activity in the plot is shown in the lower half of the 0 - 30° ring.

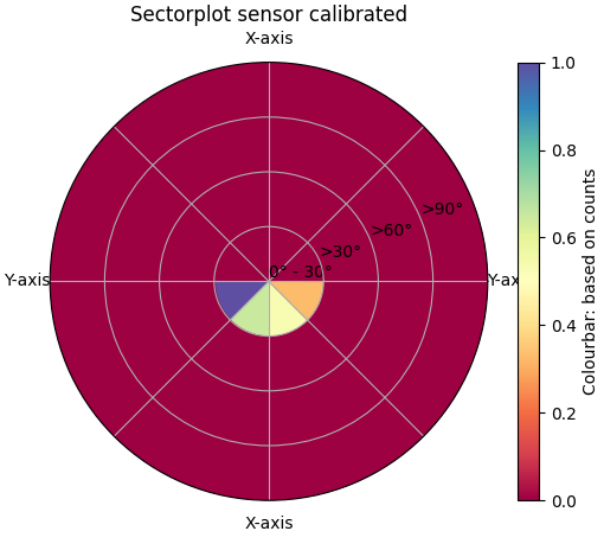

Figure 15: The sector plot of sensor-calibrated patient data of the first three hours after surgery is shown. It can be seen that the patient was in a supine position.

When comparing figures 14 and 15 with figure 16 it can be seen that the activity in the last sector plot differs significantly from the first two sector plots. This shows the linear regression algorithm does not work as effectively as with the data used in figure 13.

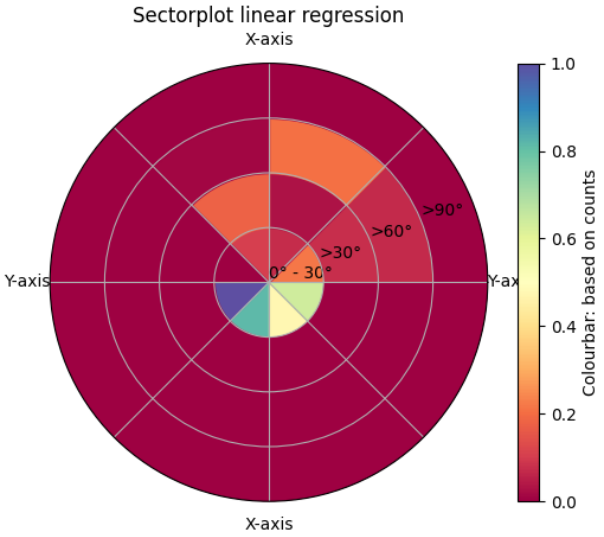

Figure 16: The sector plot of the patient data of the first three hours after surgery, which was sensor calibrated and filtered with the linear regression model, is shown. It can be seen that the patient was not in supine position all of the time.

5 Discussion

The findings of section 4 are discussed. Conclusions will be presented and evaluated. Additionally, potential imperfections in the implementation process are identified and reviewed. Lastly, possible improvements to the linear regression model are presented.

The results of the sector plots will be discussed. As presented in section 4.3 the linear regression model significantly increases the deviation from 'real life'. This means that the linear regression model as implemented in this research cannot be used for patient data. The implementation of the linear regression algorithm could be improved by the determination of the stationary periods. In this report, the results of the linear regression model are dependent on the stationary periods that were manually determined. This causes some inconsistencies when performing the calibration and linear regression process multiple times, as the stationary periods were reselected every time the script was rerun. Consequently, the α and β values of the liner regression model will differ slightly. This means that the model is not the same, every time the same data is rerun. Additionally, the number of stationary periods selected influences the result of the linear regression model. This is caused by the fact that the coefficients of the linear regression model, α and β, are redefined during every stationary period. When such a period is not selected, the values will not be updated. Lastly, stationary periods which are too small to detect or select manually, are neglected and therefore will not contribute to the bias estimation. To improve this, future research could be done to provide an algorithm, which automatically recognizes stationary periods in the gyroscopic data. In this way, the stationary periods will be the same if the process is repeated and smaller stationary periods will also be included in the gyroscope zero bias estimation. This will improve the model, as the α and β values will be calculated more accurately every stationary period will be taken into account. Furthermore, the α and β values will be updated more frequently, as no stationary periods are neglected. Algorithms for this already exist and can easily be implemented in the model used in this report. [13, 14]

As mentioned in section 4 a drift is still visible in the yaw angles after sensor calibration and application of the linear regression model. As described by Hoang et al. these angles could be optimized and the drift could be further eliminated by a no motion no integration (NMNI) filter. This filter uses stationary periods to predict the gyroscope zero bias, like the linear regression model. An algorithm can be implemented to determine the stationary periods automatically. During these stationary periods, the values of the angular velocities are set to zero and the bias is estimated. However, this bias is implemented as a constant value instead of a bias dependent on the time. [13] This filter in combination with the Madgwickfilter, which was used to obtain the orientations from the IMU data, shows a significant decrease in the drift of yaw angles. [13, 17, 18] As discussed in section 4.2 the drift is only present in the yaw angles, after application of the linear regression model. In future research, the NMNI filter could be implemented to eliminate the drift, which is present in the yaw angles.

As explained in section 4.2 the sensor calibration significantly reduces the drift of the yaw angles. Therefore, this calibration can be applied to ameliorate the approximation of the yaw angles and the sector plots of the patient data. The measurements which were used during the sensor calibration (see 3.1) used 2 different angles for different axes, i.e. 360° for the z-axis and 90° for both the x- and y-axis. This means that the calculation for the calibration values slightly differs per axis. This difference could result in slightly different calibration values and may have caused a slight drift in the yaw angles. In the future, the calibration values should be determined with the same angles used for every axis. This ensures that the values can be used together as calibration values and no distortions appear because of the calibration values.

Lastly, a recommendation for future research is to pay attention to the duration of the script. The duration of the script for the Madgwick filter of 7 hour data was an hour and a half. The sensor calibration and the linear regression model did not elongate the running time significantly. The long duration of the running of the script delays the retrieval of results significantly and this should be taken into account.

6 Conclusion

In section 1 the following research question was proposed:

To what extent can the gyroscope drift of IMUs be corrected with sensor calibration and a linear regression model?

The answer to the research question is; the gyroscope drift can be significantly reduced with a sensor calibration. However, a drift is still visible in the yaw angles. It was tried to further eliminate this drift with a linear regression model. This model showed promising results in the evaluation of the model with simulation data. Unfortunately, when evaluating the model with patient data, it was shown the model did not work as effectively and could not be used with the patient data. The linear regression model can be improved by implementing an algorithm which automatically detects stationary periods. Another way to eliminate the drift in the yaw angles after the sensor calibration is an implementation of the NMNI filter, as this filter in combination with the Madgwickfilter has shown promising results in optimizing the yaw angles of gyroscopic data.

References

[1] Aiello F, Afflitto GG, Ceccarelli F, Cesareo M, Nucci C. Global Prevalence of Fuchs Endothelial Corneal Dystrophy (FECD) in Adult Population: A Systematic Review and Meta-Analysis. Journal of Ophthalmology. 2022;2022. doi:10.1155/2022/3091695.

[2] Adamis AP, Filatov V, Tripathi BJ, Tripathi RAmC. Fuchs' endothelial dystrophy of the cornea. Surv Ophthalmol. 1993 Sep;38(2):149–168. doi:10.1016/0039-6257(93)90099-S.

[3] Tone SO, Kocaba V, Böhm M, Wylegala A, White TL, Jurkunas UV. Fuchs Endothelial Corneal Dystrophy: The Vicious Cycle of Fuchs. Prog Retin Eye Res. 2021 Jan;80:100863. doi:10.1016/j.preteyeres.2020.100863.

[4] Sridhar MS. Anatomy of cornea and ocular surface. Indian J Ophthalmol. 2018 Feb;66(2):190. doi:10.4103/ijo.IJO$_6$46$_1$7.

[5] Melles GRJ, Ong TS, Ververs B, van der Wees J. Descemet Membrane Endothelial Keratoplasty (DMEK). Cornea. 2006 Sep;25(8):987–990. doi:10.1097/01.ico.0000248385.16896.34.

[6] Chan SWS, Yucel Y, Gupta N. New trends in corneal transplants at the University of Toronto. Can J Ophthalmol. 2018 Dec;53(6):580–587. doi:10.1016/j.jcjo.2018.02.023.

[7] Maier AKB, Gundlach E, Pilger D, Rübsam A, Klamann MKJ, Gonnermann J, et al. Rate and Localization of Graft Detachment in Descemet Membrane Endothelial Keratoplasty. Cornea. 2016 Mar;35(3):308–312. doi:10.1097/ICO.0000000000000740.

[8] Parker JS, Parker JS, Tate H, Melles GRJ. DMEK Without Postoperative Supine Posturing. Cornea. 2022 Feb;42(1):32–35. doi:10.1097/ICO.0000000000003000.

[9] Roberts HW, Kit V, Phylactou M, Din N, Wilkins MR. 'Posture-Less' DMEK: Is Posturing After Descemet Membrane Endothelial Keratoplasty Actually Necessary? Am J Ophthalmol. 2022 Aug;240:23-29. doi:10.1016/j.ajo.2022.02.009.

[10] Jansen P. Acquiring Head Orientation through using an IMU with Madgwick Orientation Filtering. 2024 Mar.

[11] Barshan B, Durrant-Whyte HF. Inertial navigation systems for mobile robots. IEEE Trans Robot Automat. 1995 Jun;11(3):328–342. doi:10.1109/70.388775.

[12] Madgwick SOH. An efficient orientation filter for inertial and inertial / magnetic sensor arrays; 2010. [Online; accessed 12. Feb. 2024]. Available from: https://www.semanticscholar.org/paper/An-efficient-orientation-filter-for-inertial-and-Madgwick/bfb456caf5e71d426bd3e2fd529ee833a6c3b7e7.

[13] Hoang ML, Pietrosanto A. Yaw/Heading optimization by drift elimination on MEMS gyroscope. Sens Actuators, A. 2021 Jul;325:112691. doi:10.1016/j.sna.2021.112691.

[14] O-larnnithipong N, Barreto A. Gyroscope drift correction algorithm for inertial measurement unit used in hand motion tracking. In: 2016 IEEE SENSORS. IEEE;. doi:10.1109/ICSENS.2016.7808525.

[15] EDN. A simple calibration for MEMS gyroscopes - EDN. EDN. 2010 May. Available from: https://www.edn.com/a-simple-calibration-for-mems-gyroscopes.

[16] RMSE: Root Mean Square Error; 2024. [Online; accessed 5. Apr. 2024]. Available from: https://www.statisticshowto.com/probability-and-statistics/regression-analysis/rmse-root-mean-square-error.

[17] Hoang ML, Pietrosanto A, Iacono SD, Paciello V. Pre-Processing Technique for Compass-less Madgwick in Heading Estimation for Industry 4.0. In: 2020 IEEE International Instrumentation and Measurement Technology Conference (I2MTC). IEEE;. p. 25–28. doi:10.1109/I2MTC43012.2020.9128969.

[18] Hoang ML, Iacono SD, Paciello V, Pietrosanto A. Measurement Optimization for Orientation Tracking Based on No Motion No Integration Technique. IEEE Trans Instrum Meas. 2020 Nov;70:ArticleSequenceNumber:9503010. doi:10.1109/TIM.2020.3035571.

A List of symbols

In this appendix, a list of all the used symbols and their meaning is presented.

Symbol	Meaning
DMEK	Descemet membrane endothelial keratoplasty; the surgical procedure to transplant a part of the cornea.
EITS	Eye in the sky project; the main project this report is a part of.
FECD	Fuchs' endothelial corneal dystrophy; a condition which causes the cornea to become cloudy.
IMU	Inertial measurement unit; the sensor that is used to track head movements
RMSE	Root mean square error; a measure to evaluate the obtained results.

Table 3: List of symbols